Garca-Alonso, Javier; Maestre, David; Bartolom, Javier; Garca-Tecedor, Miguel; Vazquez-Lopez, Antonio; Taeo, Mara; Del Prado, Felix; Nogales, Emilio; Cremades, Ana

Synthesis of low dimensional oxide based complex materials by a vapor-solid method

Published in:
Oxide-Based Materials and Devices XII

DOI:
10.1117/12.2591251

Published: 01/01/2021

Document Version
Publisher's PDF, also known as Version of record

Please cite the original version:
Garca-Alonso, J., Maestre, D., Bartolom, J., Garca-Tecedor, M., Vazquez-Lopez, A., Taeo, M., Del Prado, F., Nogales, E., & Cremades, A. (2021). Synthesis of low dimensional oxide based complex materials by a vapor-solid method. In D. J. Rogers, D. C. Look, & F. H. Teherani (Eds.), *Oxide-Based Materials and Devices XII* Article 2591251 (Proceedings of SPIE - The International Society for Optical Engineering; Vol. 11687). SPIE. https://doi.org/10.1117/12.2591251

Synthesis of low dimensional oxide based complex materials by a vapor-solid method

García-Alonso, Javier, Maestre, David, Bartolomé, Javier, García-Tecedor, Miguel, Vázquez-López, Antonio, et al.

Javier García-Alonso, David Maestre, Javier Bartolomé, Miguel García-Tecedor, Antonio Vázquez-López, María Taeño, Félix del Prado, Emilio Nogales, Ana Cremades, "Synthesis of low dimensional oxide based complex materials by a vapor-solid method," Proc. SPIE 11687, Oxide-based Materials and Devices XII, 116871X (5 March 2021); doi: 10.1117/12.2591251

Event: SPIE OPTO, 2021, Online Only

Synthesis of low dimensional oxide based complex materials by a vapor-solid method

Javier García-Alonso[a], David Maestre[a], Javier Bartolomé[a], Miguel García-Tecedor[a,b], Antonio Vázquez-López[a], María Taeño[a], Félix del Prado[a,c], Emilio Nogales[a], and Ana Cremades*[a]
[a]Departament Materials Physics, Physics Faculty, Universidad Complutense de Madrid, 28040 Spain; [b]Current address: Institute of Advanced Materials (INAM), Universitat Jaume I, Avenida de Vicent Sos Baynat, s/n, 12006 Castelló de la Plana, Castellón, Spain; [c]Current address: Department of Neuroscience and Biomedical Engineering Engineered Nanosystems, Aalto University – Micronova, Espoo, Finland

ABSTRACT

Nano and microstructures of ternary oxide compounds, such as nickel gallate, indium-zinc-oxide compounds, and lithium stagnates, have been successfully synthetized by a vapor-solid method. Following this synthesis process, a significant amount of material is produced in an economic and scalable way. $NiGa_2O_4$ nano- and microneedles are grown using mixtures of Ga_2O_3 powders and Ni and Ga metallic powders as main precursors. In the case of $In_2Zn_kO_{3+k}$ compounds, the precursor blend contains ZnO and InN or In_2S_3 as a source for indium atoms, producing 1-dimensional or 2-dimentional preferential growth, respectively. The growth of complex branched structures of Li_2SnO_3 has been achieved with the use of SnO_2 and Li_2CO_3. The temperature and precursor selection allow us to engineer the size, grade of complexity and final morphology of the structures. The growth mechanism of the obtained nano and microstructures is discussed and the driven force behind it is identified as anisotropic growth, autocatalytic process and dislocation driven mechanisms, depending on the specific materials and experimental conditions. Ternary compounds will be presented together with their properties characterized by x-ray diffraction (XRD), scanning electron microscopy (SEM), energy-dispersive x-ray spectroscopy (EDS), transmission electron microscopy (TEM) and Raman spectroscopy techniques. The possibility of synthetizing nanocomposites will be also briefly discussed.

Keywords: Micro and nanostructures, ternary oxide-based compounds, growth mechanism, defects, vapor-solid method

1. INTRODUCTION

Low dimensional structures such as nanowires, nanoplates, nanoparticles and nanobelts present great advantages due to their increase surface to volume ratio and reduce size, as well as their particular morphology and properties which confer them broad applicability. Elongated nanostructures can be used as fundamental building blocks for nanotechnology applications, ranging from chemical and biological sensors, field effect transistors, to energy generation and storage devices, and more. However, for a more efficient contribution to the progress in nanotechnology, challenges regarding the physical, chemical and structural control of nanomaterials as well as the development of more complex nanostructures has to be overcome in response to modern technological demands. In order to exploit their capabilities and achieve improved performance, appropriate synthesis methods are required for the achievement of low dimensional structures with tailored morphology and composition. Recently, increasing interest is focused on the synthesis of micro and nanostructures of wide bang gap oxides such as gallium oxide[1,2], a n-type oxide with a 4.8 eV band gap with recent applications in high power technology, as well as nickel oxide[3,4], a p-type oxide with band gap around 3.8-4 eV. Other relevant oxides with reported nanostructures are also tin oxide[5], titanium oxide[6] and indium oxide[7,8]. To date, these oxides have been synthesized following a wide range of synthesis methods leading to the development of micro- and nanostructures in forms of rods, tubes, belts, and more complex morphologies. However, the quest of novel and improved functionalities requires the fabrication of materials which accomplish particular dimensions, composition and geometries, as well as high crystallinity for which a selection of adequate synthesis methods is needed. The different properties and applications of these oxide-based low dimensional structures could be improved or widened either by doping or by obtaining the ternary compounds between several of the mentioned oxides. Actually, the development of ternary compounds based on binary oxides is

*cremades@fis.ucm.es; phone +34 913944521; www.ucm.es/fine

Oxide-based Materials and Devices XII, edited by David J. Rogers, David C. Look
Ferechteh H. Teherani, Proc. of SPIE Vol. 11687, 116871X · © 2021 SPIE
CCC code: 0277-786X/21/$21 · doi: 10.1117/12.2591251

gaining increased attention as they can face challenging tasks regarding the achievement of particular composition, properties and morphology, leading in some cases to the birth of promising fields of research. This work comprises a review of diverse low-dimensional ternary compounds based on binary oxides fabricated by a vapor-solid method, alternatively by including a third element of technological interest such as Li[9] or Zn[10].

Despite the great interest aroused by low dimensional micro and nanostructures of ternary compounds, their fabrication is not an easy task and diverse synthesis approaches have been followed so far. Among these synthesis procedures, the vapor-solid method has demonstrated to be of prior choice in the fabrication of a wide variety of micro- and nanostructures of diverse ternary compounds[11,12,13]. This versatile method, which avoids the use of catalyst, templates or external substrate, requires a precise control of different parameters which govern the growth of the micro- and nanostructures in a scalable way. Regarding the synthesis of ternary compounds, special attention has to be paid to the selected precursors and the temperature and duration of the thermal treatment in order to achieve a tailored composition of the as-grown microstructures. Besides, different mechanisms[14,15] could be involved during the vapor-solid growth, such as self-catalytic growth, dislocation-driven growth and anisotropic growth. The driving-force leading to the growth of the different low dimensional structures based on ternary compounds by a vapor-solid method are not completely understood so far. In this work, different micro- and nanostructures from diverse ternary compounds grown by a vapor-solid method are described and the driven forces governing the growth mechanisms are discussed as well.

The spinel structure is a common one for complex materials, which leads to a variability of behaviors and applications due to the accommodation of cations with different sizes and charge states[16]. An inverse spinel structure is the one of the $NiGa_2O_4$ samples under study in this work. As for other transition metal spinels, it exhibits luminescence properties, and it is also adequate for photocatalysis applications[17]. $NiGa_2O_4$ has been mainly synthetized in the form of nanoparticles[18], however less has been done so far in the fabrication of elongated micro- and nanostructures, as those described in this work.

As a critical raw material In presents supply risks that have prompted the search for alternative materials to In_2O_3 or indium tin oxide (ITO), with a lower content of this element. One of the most promising materials for the substitution of ITO as transparent electrode is the In_2O_3-ZnO system, also known as IZO. This system is characterized by the formation of ternary $In_2Zn_kO_{k+3}$ homologous compounds, with k integer, when the Zn content is above the solubility limit of 2 % atomic. The properties of these compounds are close to those of ITO, but with the advantage of a lower In content. Besides, they also present some other distinctive characteristics such as a high Seebeck coefficient or a low thermal conductivity[19], which are desirable from the thermoelectric applications point of view. IZO single crystalline nano or microstructures are scarcely reported[20] and the complex structure[21] of this material is still under study.

The Sn-based ternary compound Li_2SnO_3 is commonly used in applications related to the fabrication of electrodes for Li-ion batteries[22], as well as in catalysis and in the fabrication of dielectric materials for microwaves[23]. Despite these applications, Li_2SnO_3 is a poorly studied material, mainly due to the necessity of adequate synthesis methods, and many of its physical properties are still unknown or under discussion, as for example its fundamental band gap.

Besides, the fabrication of composite material using either ternary compounds or binary oxide nanomaterials as a filler in a polymeric or carbonaceous matrix can also lead to improved performance, as advantage can be taken from their easy processing, low cost and possibility to be a part of flexible devices with tuneable properties.

The purpose of this article is to review some of the research results achieved in our group related to the obtention of nano- and microstructures of ternary complex oxides with interesting technological applications. In this work, micro and nanostructures of Ni gallate, IZO and Li stagnate ternary compounds synthetized by vapor-solid will be presented together with some of their properties characterized by x-ray diffraction (XRD), scanning electron microscopy (SEM), energy-dispersive x-ray spectroscopy (EDS), transmission electron microscopy (TEM) and Raman spectroscopy techniques. The selection of experimental conditions allows us to engineer the size, grade of complexity and final morphology of the structures. The growth mechanisms of the obtained nano- and microstructures will be discussed and the driven force behind it identified. Some practical issues about obtaining nanocomposites with oxide-based materials will be briefly described.

2. EXPERIMENTAL

The samples have been fabricated by a thermal treatment of a precursor pellet. The pellet is made of a pressed mixture of oxides (Ga_2O_3, ZnO, SnO_2), metals (Sn, Ni, Ga) or other precursors such as lithium carbonate, indium sulfide or indium nitride as shown in the Table 1. The pellet is annealed under a dynamic atmosphere of Ar up to 1500 ºC depending on each material and the selection of precursors. Usually, a treatment in a single step is used, maintaining the temperature stable for 5 to 10 hours. Sometimes a two-step treatment is preferred if taken advantage from the different sublimation rates of the precursors is seek. The micro and nanostructures are form on the pellet surface that acts simultaneously as substrate and as source of material, avoiding the use of catalysts, templates and external substrates, by a vapor-solid mechanism.

Table 1. Experimental conditions used to synthesize the nano and microstructures.

Material	Precursors	Temperature (duration)
$NiGa_2O_4$	Ga_2O_3, Ni and Ga	1400 ºC (10h) 1500 ºC (10h)
IZO	InN or In_2S_3 and ZnO	700 ºC (5h)-900 ºC (5h)
Li_2SnO_3	Li_2CO_3 and SnO_2	700 ºC (5h) 800 ºC (5h) 900 ºC (5h)

In most cases, the ternary compounds fabricated following this method coexist with other oxides appeared in the surface of the pellet on top of which the micro- and nanostructures grow. Hence, some of the as-grown low-dimensional structures can be detached from the pellet and placed onto Si substrates in order to perform an individual analysis.

The micro and nanostructures have been characterized by SEM, XRD, TEM and Raman spectroscopy. The morphological and the compositional analysis were obtained using a scanning electron microscope (SEM, Leica 440 Stereoscan) equipped with an EDX Bruker AXS 4010 analyzer to provide the energy dispersive X-ray spectroscopy (EDS) results. X-ray diffraction (XRD) was carried out with a PANanalytical X'Pert Powder equipment, using the Cu Kα line. Raman measurements were carried out by means of a confocal microscope Horiba Jobin-Yvon LabRam HR800 using a He-Cd (325 nm) or a 633 nm He–Ne laser as excitation source. The microstructural analysis was performed in a transmission electron microscope JEOL JEM 3010 operated at 300 kV.

3. RESULTS AND DISCUSION

3.1 Nickel Gallate

The micro and nanostructures are grown at 1500 ºC and 1400 ºC, hereinafter also referred as Sample A and B, respectively. In Figure 1, the SEM images show representative structures of both samples, mainly in form of nanoneedles and microrods, covering with a high density the surface of the pellet. The main differences between the structures grown at 1500 and 1400 ºC are related to a bigger size for the ones grown at lower temperature with a reduce density of them on the pellet surface. The elongated microstructures show lengths up to tens of microns and widths of some microns or even hundreds of nm. Most of the bigger needles are faceted with a hexagonal section, such as the one shown in Figure 1(b), which shows a terraced appearance of the lateral faces.

By gently detaching the structures, single isolated ones can be study in more detail. Some of the needles exhibit at the top a small droplet, which can be observed at higher magnifications. Only in some rods of the sample grown at a reduced temperature, bigger droplets are observed. In Figure 2a, a needle shows a reduction of the section or tapering towards the tip due to the consumption of the catalyst droplet during the growth. Taking into account the cubic spinel structure of this compound, the preferential growth in a specific direction cannot be justified by the anisotropic growth originated by the minimization of surface energy of different crystalline orientations as they would be quite similar due to the isotropic nature of the cubic structure. This is an indication of the autocatalytic vapor-liquid-solid (VLS) growth mechanism which is assisted by the presence of metallic Ga and Ni in the precursors. The EDS mappings of Figure 2b show that these final droplets present a Ni enrichment as compared to the rod. The average composition of the samples detected by EDS shows that the ratio of Ga to Ni is around 2 with an excess of Ga, and slightly increasing from the base to the top, which reflects the different incorporation rates of Ni and Ga from the catalyst into the final crystal.

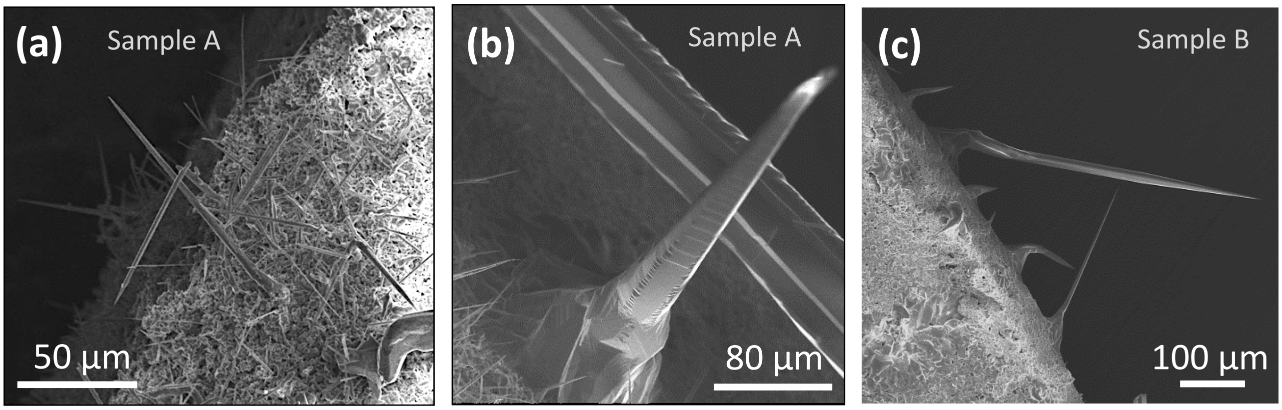

Figure 1. SEM images of the nano and microstructures of $NiGa_2O_4$ grown at (a) and (b) 1500 ºC and (c) 1400 ºC

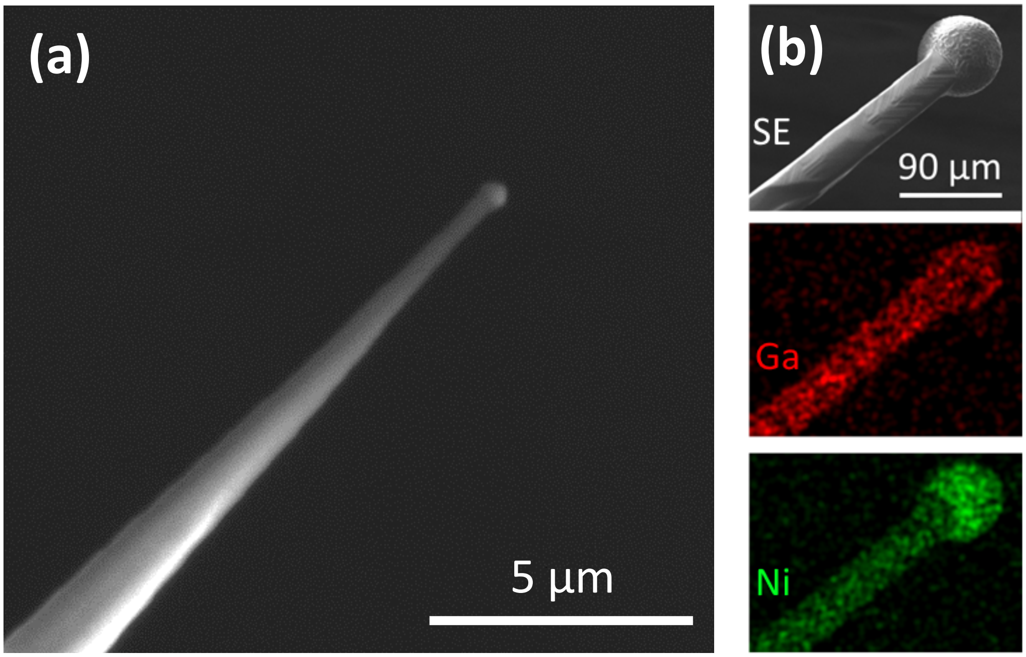

Figure 2. (a) SEM image showing the droplet at the top of a microneedle and (b) SEM image and EDS mapping of one microrod of the sample grown at 1400 ºC.

XRD analysis, not shown here, confirms the presence of Ga_2O_3 and $NiGa_2O_4$ in the treated pellets. As shown in Figure 3, the characterization of isolated rods enables the identification from the Raman spectra of their Ni gallate structure in agreement with the literature[24]. The peaks do not correspond to the well-known spectrum of Ga_2O_3, which is also included in the Raman figure as a reference. The dominant Raman mode corresponds to the A_{1g} mode centered at around 744 cm^{-1}, while E_g and T_{2g} modes are centered at 533 and 616 cm^{-1}, respectively. The assignment of peaks to specific modes is however tentative as the work is ongoing, hence further study is still required in order to gain deeper insight in the understanding of the vibrational modes from this ternary compound. In the Raman spectra of different nano and micro rods the same features are observed for all the probed samples whether they are detached from sample A, or B, with nano or micrometric sizes or even when the spherical particle at the top of the structures has been probed. In this case the only differences are a slight shift of the A_{1g} peak towards higher energy related to the higher amount of nickel in the ending spherical tip, as measured by EDS, and a small shoulder in the A_{1g} mode for the rods of the sample grown at higher temperature.

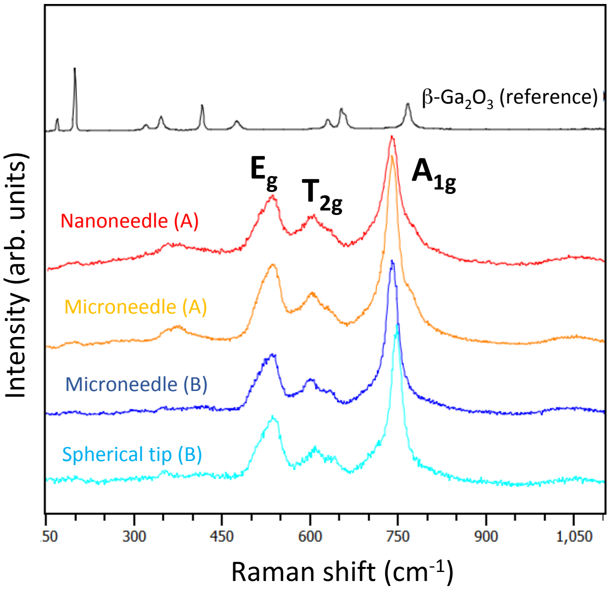

Figure 3. Raman spectra of single rods from sample A and B. Spectrum from Ga_2O_3 is also included as a reference.

3.2 Indium zinc oxide

Indium zinc oxide homologous compounds are complex materials with a structure consisting of alternate layers of InO_2 octahedra and wurtzite-like $InZn_kO_{k+1}$ stacked perpendicular to the c-axis of the crystal, where zinc and indium occupy tetrahedral and trigonal bipyramid sites[25]. The structure of this material has been studied in detail by different authors[21,26]. An interesting feature of the IZO heterostructure is a structural modulation in the form of a zig-zag pattern related to an inhomogeneous In distribution in the In/Zn–O blocks, which is observed not only for high k terms as previously proposed, but also for lower k members as demonstrated in our previous work[21]. In a first approximation, the origin of the modulation is attributed to the confinement of the wurtzite blocks inside the InO_2 layers, which causes a gradual displacement of the anion sublattice along the In/Zn-O blocks inverting the polarization and allowing the formation of the superlattice. The indium atoms arrange themselves in the most stable configuration inside the blocks following a zig-zag pattern. This zig-zag pattern is however not found in samples incorporating doping elements such as Ga and Al, as reported in a recent work[27]. Therefore, the properties of these homologous compounds usually depend on the k term and can be modulated by dopant incorporation, as reported for the Raman and luminescence emission[21,27] and also for the electrical conductivity[28] and calculated band gaps[29].

Obtaining micro and nanostructures of IZO is of technological interest, as an alternative material to In_2O_3 or ITO, and due to new applications as a thermoelectric material[30]. In this work, the growth mechanism involved in the final morphology and dimensionality of the micro and nanostructures is shown to be dependent on the selection of different precursors. A mixture of InN or In_2S_3 and ZnO have been used as precursors to fabricate the micro and nanostructures of IZO. In this case, a two-step treatment is used[10,20,31]. For convenience the samples including indium nitride will be referred to as N samples whereas those including indium sulfide will be named as S samples. The use of different precursors allows the obtention of different dimensionalities due to the activation of different growth modes.

In the N samples the thermal treatments lead to the growth of elongated structures mainly rods and needles, as well as hierarchical structures presenting different levels of ordering. The needles show a Zn content of few atomic percent distributed quite homogenously along the structures. Local EDS measurements on the rod axis show that the incorporation of Zn increases towards the top and this fact is related to an increase of the cathodoluminescence (CL) intensity as well as a band broadening observed with Zn incorporation. In the most developed structures secondary growth is observed showing also the gradient in the zinc concentration, as observed before (see Figure 4a). The higher CL emission is also related with the Zn incorporation. The different rate of sublimation for the components of the initial mixture is a necessary requirement for the development of these hierarchical structures that tend to grow at the top regions of the rods. The core of the rod is however grown by a dislocation-driven growth[7,31]. Dopant segregation at the surface of the central rod may lead to the lateral growth of these structures. IZO formation can be assessed by a number of techniques, namely XRD, TEM, Raman or cathodoluminescence/photoluminescence. The size of the structures makes XRD and TEM unsuitable for their direct study, but CL measurements (Figure 4b) show an overlapped emission of In_2O_3 luminescence, originated at the core of the rods, mixed with characteristic IZO emission form the surface of the structures.

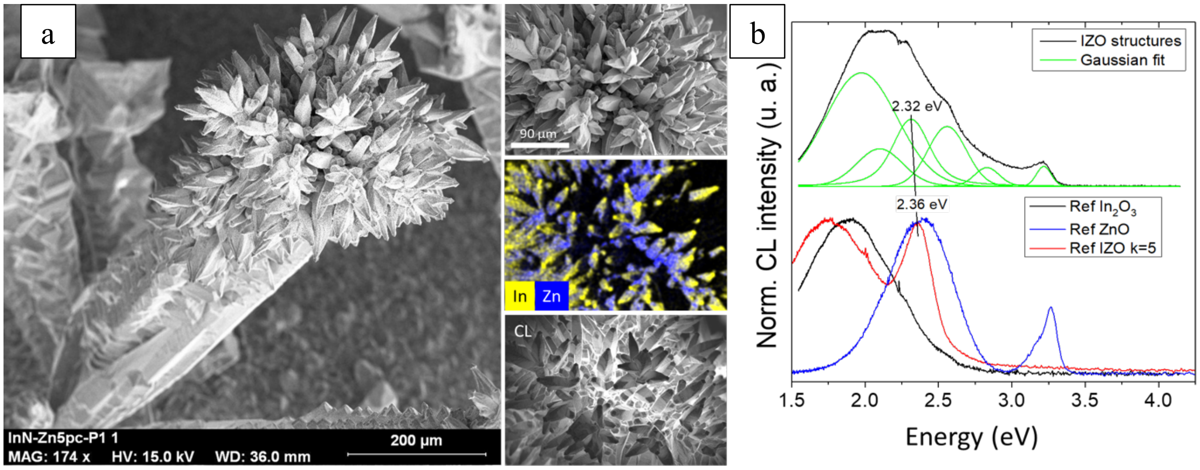

Figure 4. (a) Example of IZO hierarchical structures grown from InN precursor, showing the inhomogeneous incorporation of Zn and its influence on the luminescence of the structures. (b) Representative CL emission of the IZO structures showing the gaussian fit and comparison to reference ZnO, In_2O_3 and IZO powders. The spectrum is a mixture of In_2O_3 (from the core) and IZO (at the surface) emission.

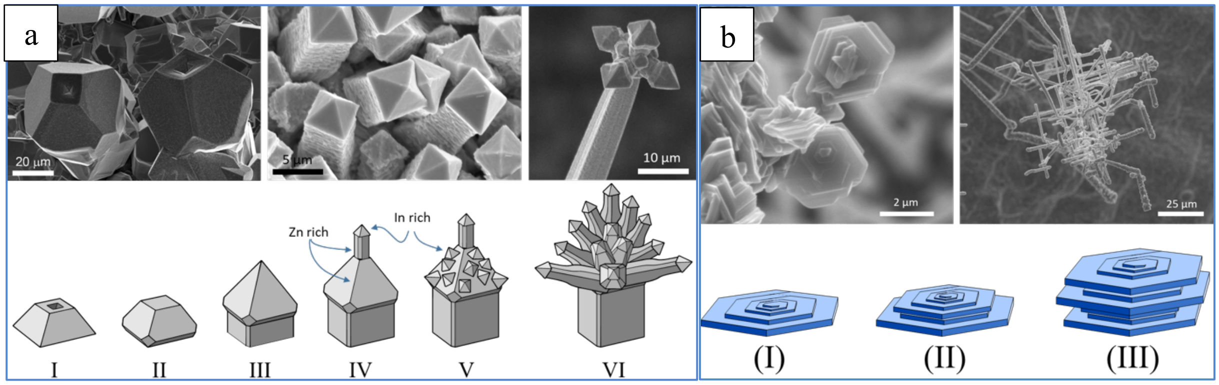

Figure 5. (a) Growth model for IZO elongated. When InN is used as precursor, complex hierarchical elongated structures are obtained as the result of different sublimation rates of In/Zn. (b) Growth model for two-dimensional micro and nanostructures. When In_2S_3 is used as precursor, 2D plate stacks are obtained via a screw dislocation driven growth process.

For the S samples two-dimensional structures are obtained with different morphologies as plates and stacks, some of them organized hierarchically as observed in Figure 5. The thickness of the plates is of few hundreds of nanometers. There are also some rods which develop plates on their surface as a result of secondary growth.

The stacks of plates grow by a dislocation driven growth, which have been demonstrated in the last years for several plates, nanowires and nanotubes of different materials[32,33]. The hexagonal plates contained helical steps at the surface showing the presence of dislocations. The two-dimensional dislocation-driven growth could be explained by a comparable growth rate of steps at the dislocation core and at the outer edge of the plate. On the contrary, if the growth rate at the core steps is higher than that at outer regions, due to impurity pinning points or slower transport kinetics, the growth of 1D structures is favored. The relative growth rates, in the nanoplate plane and in the perpendicular direction can change during the growth due to different adsorption rates at the steps or to variations of transport kinetics during growth, therefore the growth can alternate between two-dimension and one-dimension modes. As a result, stacks of nanoplates joined by a central axis are obtained.

3.3 Lithium stagnate

Novel morphologies have been achieved for Li_2SnO_3, leading to potential extended applicability of this material usually employed in the field of energy storage so far. Mainly Li_2SnO_3 branched structures have been obtained at 700 and 800 ºC by a vapor-solid method. As an example, the high number of structures obtained at 800 ºC are shown in Figure 6(a), (b) and (c). EDS results show a homogenous distribution of tin and oxygen in the probed structures (not shown here). In this case, lithium has been detected by XPS (not shown here) and also by electron energy loss spectroscopy (EELS) as shown in the spectra of Figure 7(a). As confirmed by Raman spectroscopy (not shown here) and selected area electron diffraction (SAED) measurements performed on individual nanostructures, as the one of Figure 7(b) for samples grown at 800 ºC, the samples grown at 900 ºC are complex SnO_2/Li_2SnO_3 core-shell elongated microstructures whereas the structures obtained at 700 and 800 ºC exhibit only the Lithium stagnate phase.

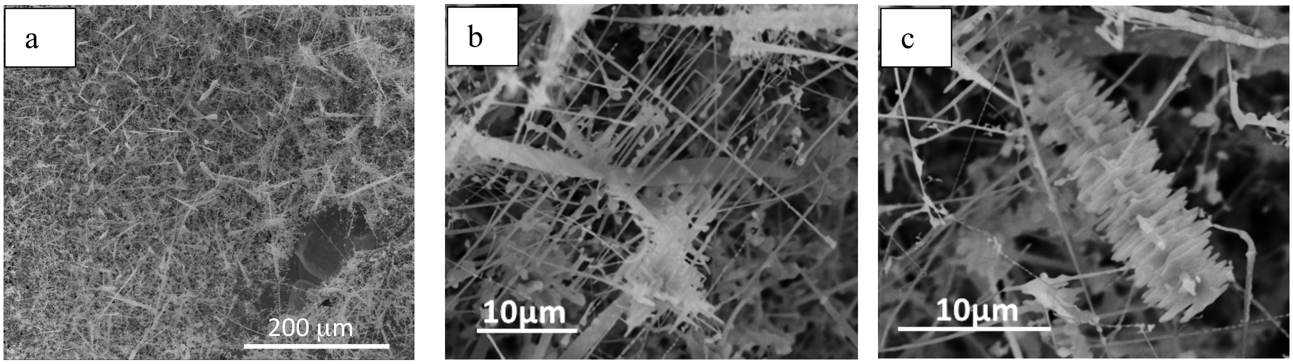

Figure 6. (a), (b) and (c) SEM images of structures synthetized at 800 ºC at different magnifications.

As observed in the TEM images stacking faults along the central stem along the [001] direction are revealed in agreement with the diffuse streaks clearly observed in the [110] SAED pattern (Figure 7b). The presence of structural disorder associated with stacking faults along c-axis in Li_2SnO_3 crystals has already been studied by Tarakina[34,35] and are related to a the low-temperature (LT)-phase, formed at temperatures below 800 °C, whereas a high temperature phase (HT)-Li_2SnO_3, would be formed at temperatures above 1000 ºC. Both phases are monoclinic but exhibit slightly different lattice parameters. In both cases the oxygen atoms form a distorted cubic network with octahedral positions occupied by Li^+ and Sn^{4+} cations. The extremely high white luminescent emission observed in some samples, not shown here, could enhance their functionality in phosphor-free white light-emitting devices.

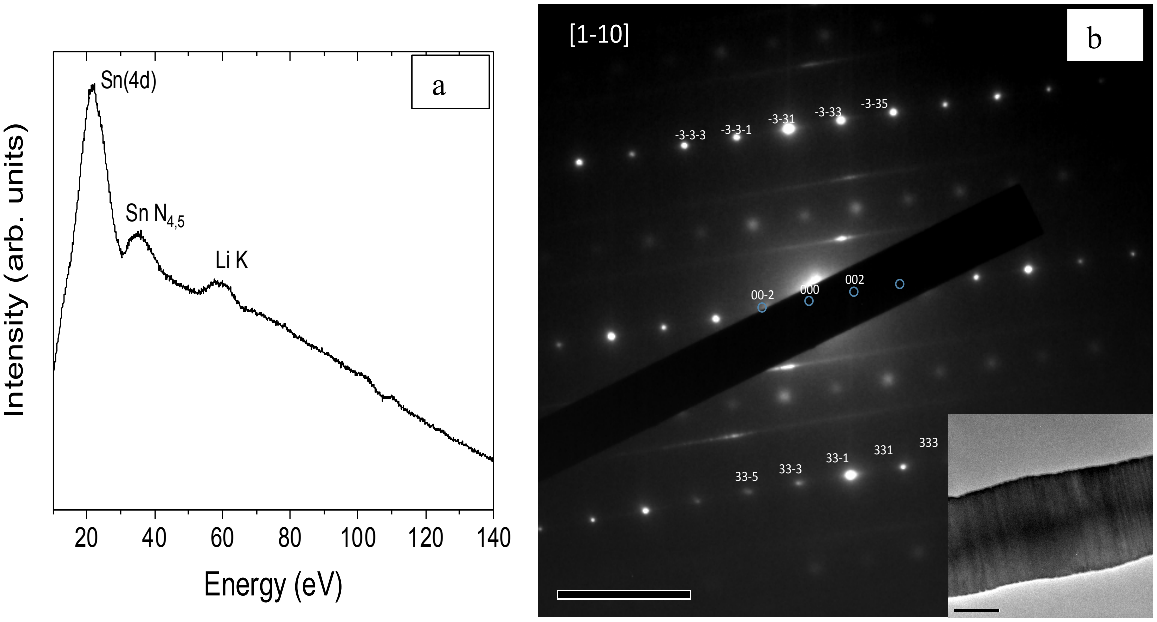

Figure 7. (a) EELS spectrum which confirms the presence of Li in the structures. (b) SAED pattern confirms the formation of the Li_2SnO_3 phase. Streaking lines parallel to the growth direction are distinctive of stacking disorder and stacking fault formation, (clearly visible on the inset), characteristic of the low temperature Li_2SnO_3 phase.

3.4 Oxide based composites

Nanocomposites are also considered as complex materials as these are defined as nanostructured materials with combinations of structure and/or composition that lead to performance surpassing the sum of their individual components. Nanocomposites with hosts such as polymers or carbon derivatives and oxide-based nanostructures as filler will widen the applicability of the oxide materials in a series of fields. As a matter of fact, the composite formation improves the performance of the single counterparts, including new functionalities as well. The nanocomposite is also a medium which could be easier to manipulate, contact or process as a layer, offering significant advances in the implementation of the nanostructures.

The oxide material used as a filler in the composite may be a transparent conductive oxide (TCO) such as Ga_2O_3, SnO_2, TiO_2 or NiO, undoped or doped with different elements or a ternary compound. The nanostructures could exhibit different dimensionalities, but the realization of homogenous films, e. g. with a polymer host by spin-coating, is best achieved by using nanoparticles of reduced sizes, which are usually synthetized by soft chemical methods. In this sense, some additives have proved to be useful such as ethylene glycol (EG), dimethyl sulfoxide (DMSO) or Triton, in order to avoid agglomeration, to improve substrate wettability and other properties such as electrical conductivity[36]. Some examples of these nanocomposites have been developed by our group in relation with applications in energy such as Li ion batteries[37,38] solar cells[36,39,40,41] or white lighting devices[42] and presently we are also working in developing sensor capabilities with different designs using composites as well as single vapor-solid structures. The incorporation into a film of nanostructures grown by a vapor-solid method, mainly presenting elongated morphologies, is still challenging due to agglomeration issues, or the lack of orientation of the filler. However, the random orientation of nanowires or nanotubes inside the host could be both of advantage and disadvantage depending on the specific application, so that further research work should be carried out to progress on the implementation of these nanostructures. As a matter of fact, new processing techniques such as the additive manufacturing could be used to fabricated polymer-based nanocomposites reinforced by nanofibers with good results.

4. CONCLUSIONS

Following a vapor-solid growth oxide-based ternary compound micro and nanostructures are successfully synthetized. Examples of different structures with one- or two-dimensional morphologies have been shown for $NiGa_2O_4$, IZO and Li_2SnO_3. The selection of the adequate experimental conditions such as temperature, one or two-step treatments, as well as the precursor powders are key factor to engineer the size, morphology and final composition. The detail study of the micro and nanostructures allows to identify the growth driven force behind the process. Anisotropic growth, autocatalytic growth or dislocation driven growth are described for these structures.

5. ACKNOWLEDGEMENTS

This work was supported by MINECO/FEDER/M-ERA.Net Cofund projects: RTI2018-097195-B-I00 and PCIN-2017-106.

REFERENCES

[1] M.Alonso-Orts, G. Chilla, R. Hötzel, E. Nogales, J.M. San Juan, M. L. Nó, M. Eickhoff, and Bianchi Méndez, Optics Letters 46 (2), 278-281 (2021)
[2] P. Feng, J. Y. Zhang, Q. H. Li, and T. H. Wang, Appl. Phys. Lett. 88, 153107 (2006)
[3] M. Taeño, D. Maestre, A. Cremades, Materials Letters 271, 127801 (2020)
[4] Q.Yang, J. Shaa, X. Ma, D.Yan, Materials Letters 59 (14–15), 1967-1970 (2005)
[5] M. García-Tecedor, D. Maestre, A. Cremades, J. Piqueras, The Journal of Physical Chemistry C 120 (38), 22028-22034 (2016)
[6] D. Maestre, A. Cremades, L. Gregoratti, and J. Piqueras, Journal of Nanoscience and Nanotechnology 8, 1–5, (2008)
[7] J. Bartolomé, A. Cremades, J. Piqueras, J. Mater. Chem. C 1, 6790–6799 (2013)
[8] P. Guo, R. P. H. Chang, R. D. Schaller ACS Photonics 4, 1494−1500 (2017)
[9] F. del Prado, A. Cremades, D. Maestre, J. Ramírez-Castellanos, J.M. González-Calbet, and J. Piqueras, Journal of Materials Chemistry A 6 (15), 6299-6308 (2018)
[10] J. Bartolomé, D. Maestre, A. Cremades, M. Amatti, J. Piqueras, Acta materialia 61 (6), 1932-1943 (2013)
[11] J. Dolado, K.L. Renforth, J.E. Nunn, S.A. Hindsmarsh, P. Hidalgo, A.M. Sańchez, and B. Méndez, Cryst. Growth Des. 20(1), 506–513 (2020)
[12] I. López, E. Nogales, B. Méndez, J. Piqueras, A. Castaldini and A. Cavallini, Materials Research Express 1(2),025017 (2014)
[13] C. He, Q. Wu, X. Wang, Y. Zhang, L. Yang, N. Liu, Y. Zhao, Y. Lu, and Z. Hu ACS Nano 5(2), 1291–1296 (2011)
[14] A. Cremades, M. Herrera, J. Bartolomé, G.C. Vásquez, D. Maestre, J. Piqueras, Physica B: Condensed Matter 453, 92-99 (2014)
[15] M. García-Tecedor, F. del Prado, C. Bueno, G. C. Vásquez, J. Bartolomé, D. Maestre, T. Díaz, A. Cremades, and J. Piqueras, AIMS Materials Science 3(2), 434-447 (2016)
[16] A. Navrotsky and O. J. Keppa, J. Inorg. Nucl. Chem. 30, 479 (1968)
[17] L. Chen, T. Horiuchi and T. Mori, Appl. Catal. A Gen. 209, 97 (2001)
[18] Y. Huang, J. Ouyang, X. Tang, Y. Yang, J. Qian, J. Lu, L. Xiao, and L. Zhuang ACS Applied Materials & Interfaces 11 (8), 8025-8031 (2019)
[19] L. Fang, X.F. Yang, L.P. Peng, K. Zhou, F. Wu, Q.L. Huang, C.Y. Kong, J Supercond Nov Magn 23, 889–892 (2010)
[20] J. Bartolomé, D. Maestre, M. Amati, A. Cremades, J. Piqueras, J. Nanopart. Res. 15, 2015 (2013)
[21] J. García-Fernández, J. Bartolomé, A. Torres-Pardo, A. Peche-Herrero, J. Moreno, J. Ramírez-Castellanos, A. Cremades, J. M. González-Calbet, J. Piqueras. J. Mater. Chem. C 5, 10176-10184 (2017)

[22] Q. F. Wang, Y. Huang, J. Miao, Y.Wang, Y. Zhao, Appl. Surf. Sci. 258, 6923–6929 (2012)

[23] Z. F. Fu, P. Liu, J. L. Ma, B. C. Guo, X. M. Chen, H. W. Zhang, Mater. Res. Bull. 77, 78–83 (2016)

[24] X. Ma, C.Wang, G. Wang, G. Li, S. Li, J. Wang, and Y. Song, Journal of Industrial and Engineering Chemistry 66, 141-157 (2018).

[25] C. Li, Y. Bando, M. Nakamura, N. Kimizuka, J. Electron Microsc. 46, 119-127 (1997)

[26] W. Yu, W. Mader, Ultramicroscopy 110, 411–417(2010)

[27] J. García-Fernández, A. Torres-Pardo, J. Bartolomé, R. Martínez-Casado, Q. Zhang, J. Ramírez-Castellanos, O. Terasaki, A. Cremades, J. M. González-Calbet, Chem. Mater. 32, 6176−6185 (2020)

[28] T. Moriga, D. D. Edwards, T. O. Mason, G. B. Palmer, K. R. Poeppelmeier, J. L. Schindler, C. R. Kannewurf, I. Nakabayashi J. Am. Ceram. Soc., 81(5), 1310–16 (1998))

[29] A. Walsh, J. L. F. Da Silva, Y. Yan, M. M. Al-Jassim, S.-H. Wei, Phys. Rev. B 79, 073105 (2009)

[30] T. Moriga, K. Ishida, K. Yamamoto, A. Yoshinari, K.-I. Murai, Mater. Res. Innovations 13, 348-351 (2009)

[31] J Bartolomé, D Maestre, M Amati, A Cremades, J Piqueras The Journal of Physical Chemistry C 115 (16), 8354-8360 (2011)

[32] S. A. Morin, A. Forticaux, M. J. Bierman, S. Jin, Nano Lett. 11, 4449–4455 (2011)

[33] D. Maestre, D. Häussler, A. Cremades, W. Jäger, J. Piqueras J. Phys. Chem. C 115, 18083–18087 (2011)

[34] N. V. Tarakina, T. A. Denisova, Y. V. Baklanova, L. G. Maksimova, V. G. Zubkov, R. B. Neder, Adv. Sci.Technol. 63, 352–357 (2010)

[35] N. V. Tarakina, T. A. Denisova, L. G. Maksimova, Y. V. Baklanova, A. P. Tyutyunnik, I. F. Berger, V. G. Zubkov, G. Z. Van Tendeloo, Kristallogr. Suppl. 2009, 30, 375–380

[36] H A. Vázquez-López, A. Yaseen, D. Maestre, J. Ramírez-Castellanos, S. Karazhanov, E. S. Marstein and A. Cremades, Materials Letters 271, 127802 (2020)

[37] A. Vázquez-López, D. Maestre, J. Ramírez-Castellanos, J. M. González-Calbet, I. Píš, S. Nappini, N. Yuca and A. Cremades, Journal of Physical Chemistry C 124 (34), 18490-18501 (2020)

[38] F. del Prado, H. F. Andersen, M. Taeño, J.P. Mæhlen, J. Ramírez-Castellanos, D. Maestre, S. Karazhanov and A. Cremades, Scientific Reports 10, 5503 (2020)

[39] D. Moldarev, M. Taeño, D. Maestre, A. Cremades, S. Karazhanov and E. Marstein, Materials Today Proceedings 33, 2499–2502 (2020)

[40] A. Vázquez-López, A. Yaseen, D. Maestre, J. Ramírez-Castellanos, E. Marstein, S. Zh. Karazhanov, A .Cremades
Molecules 25(3), 695 (2020)

[41] M.García-Carrión, J. Ramírez-Castellanos, E. Nogales, B. Méndez, C.C.You, S. Karazhanov, and E.S. Marstein, Mater. Lett. 2020, 261, 127088.

[42] F. del Prado, M.Taeño, D. Maestre, J. Ramírez-Castellanos, J.M. González-Calbet and A. Cremades, Journal of Physics and Chemistry of Solids 129, 133-139 (2019)